Am J Nucl Med Mol Imaging 2021;11(6):519-528
www.ajnmmi.us /ISSN:2160-8407/ajnmmi0139826

Original Article

The use of ^{68}Ga-EDTA PET allows detecting progressive decline of renal function in rats

Andrea O Fontana[1], Mary Gonzalez Melo[2], Gilles Allenbach[1], Costa Georgantas[1], Ruijia Wang[1], Olivier Braissant[3], Frederic Barbey[4], John O Prior[1], Diana Ballhausen[2], David Viertl[1]

[1]Department of Nuclear Medicine and Molecular Imaging, Lausanne University Hospital and University of Lausanne, CH-1011 Lausanne, Switzerland; [2]Paediatric Metabolic Unit, Pediatrics, Woman-Mother-Child Department, University of Lausanne and University Hospital of Lausanne, Switzerland; [3]Service of Clinical Chemistry, Lausanne University Hospital and University of Lausanne, CH-1011 Lausanne, Switzerland; [4]Department of Immunology, Lausanne University Hospital and University of Lausanne, CH-1011 Lausanne, Switzerland

Received October 14, 2021; Accepted November 8, 2021; Epub December 15, 2021; Published December 30, 2021

Abstract: Introduction: Evaluation of glomerular filtration rate is very important in both preclinical and clinical setting, especially in the context of chronic kidney disease. It is typically performed using ^{51}Cr-EDTA or by imaging with ^{123}I-Hippuran scintigraphy, which has a significantly lower resolution and sensitivity as compared to PET. ^{68}Ga-EDTA represents a valid alternative due to its quick availability using a ^{68}Ge/^{68}Ga generator, while PET/CT enables both imaging of renal function and accurate quantitation of clearance of activity from both plasma and urine. Therefore, we aimed at investigating the use of ^{68}Ga-EDTA as a preclinical tracer for determining renal function in a knock-in rat model known to present progressive decline of renal function. Methods: ^{68}Ga-EDTA was injected in 23 rats, either wild type (n=10) or knock-in (n=13). By applying a unidirectional, two-compartment model and Rutland-Patlak Plot linear regression analysis, split renal function was determined from the age of 6 weeks to 12 months. Results: Glomerular filtration ranged from 0.025±0.01 ml/min at 6 weeks to 0.049±0.05 ml/min at 6 months in wild type rats. Glomerular filtration was significantly lower in knock-in rats at 6 and 12 months ($P<0.01$). No significant difference was observed in renal volumes between knock-in and wild type animals, based on imaging-derived volume calculations. Conclusions: ^{68}Ga-EDTA turned out to be a very promising PET/CT tracer for the evaluation of split renal function. This method allowed detection of progressive renal impairment in a knock-in rat model. Additional validation in a human cohort is warranted to further assess clinical utility in both, healthy individuals and patients with renal impairment.

Keywords: Glomerular filtration rate, renal plasma function, rutland-patlak plot, positron emission tomography, gallium-68 EDTA

Introduction

Kidneys play a fundamental role in the excretion of toxic metabolites into the urine as well as a regulator of various other physiological functions. The glomerular filtration rate (GFR) is widely considered the best overall index of kidney function and has a very important clinical value in detecting and preventing kidney disorders in both, healthy and ill patients [1]. Several different approaches are available to estimate the renal capacity, with serum and urine creatinine levels being the most current and practical one [2, 3]. Nowadays, various nuclear medicine techniques are available for the characterization of renal function. Hippuric acid-based SPECT (Single Photon Emission Computed Scintigraphy) has represented an important diagnostic tool to evaluate GFR measurements since its introduction, and ^{123}I-Hippuran has been used for renal scintigraphy for many years [4]. Ortho-Hippuric acid is filtered by the glomerulus and furthermore eliminated by tubular excretion, therefore representing a valuable tool to assess renal plasma flow (RPF). Historically, single-photon-emitting radiotracers, in particular ^{99m}Tc-labeled mercaptoacetyltriglycine (MAG3), excreted mostly by tubular secretion but also by glomerular filtration [5] and diethylenetriaminepenta-ace-

tate (DTPA), which is purely filtered by the glomerulus, have been the gold standard for imaging glomerular filtration since their introduction[6]. However, conventional renal imaging using scintigraphy is characterized by relatively low spatial resolution, resulting in imaging with imprecise anatomic correlation. Using combined SPECT/CT allows enhancing imaging resolution, but needs longer acquisition times, which is a significant limitation for proper renal imaging [6]. In recent years, there has been a notable development of positron emission tomography (PET) agents for renal imaging, with several agents reaching clinical use [7]. Compared to SPECT/CT, PET/CT offers accurate camera-based quantification, which is considered superior to the current γ-camera technology, enabling imaging and quantification of renal function. Most importantly, as compared to conventional SPECT, count rates obtained by PET are significantly higher. This allows administration of significantly less radioactivity, rendering this technique safer and suitable for pediatric applications [8].

Gallium-68-labeled ethylenediaminetetraacetate (EDTA) was demonstrated to be a very promising PET-tracer for the estimation of renal function. It was first used by Hofmann and Hicks [9] to assess split renal function (SRF), and its efficacy has now been showed in a clinical trial [10]. As ^{68}Ga-EDTA is only filtered by the glomerulus, but not further secreted or resorbed at the tubular level, it allows proper assessment of glomerular filtration rate. Normally, after intravenous administration, the radiotracer initially concentrates in the blood pool, which makes it possible to use the aorta or the heart volume in order to provide input functions for kinetic analysis of distribution. Over time, the activity increases in the renal cortex to gradually flow into the renal parenchyma and from there into the bladder, where the activity starts to accumulate few minutes after injection. Although ^{68}Ga-EDTA has been used in the context of pathological brain imaging [11], its clinical use in renal disease has been limited to a few selected preclinical and clinical studies [10, 12]. Therefore, investigating the use of ^{68}Ga-EDTA in pathological kidney conditions may represent a promising line of research.

To determine split renal function, which is defined as the relative contribution of each of the two kidneys to total renal function, two mathematical methods are typically used, namely the integral method, or area under the curve (AUC) and the Rutland-Patlak plot [13, 14]. The AUC methodology is based on the ratio between the activity in the bladder at the end of the acquisition time and the area under the glomerulo-tubular curve for each kidney [15]. The Rutland-Patlak plot describes a graphical solution of a simplified two-compartment model, which inherently assumes that the rate of change of tracer concentration in the kidneys is constant during the clearance phase (**Figure 1A**) [16]. It is typically preferred to the AUC methodology as it has shown to be more reproductible [17, 18].

Several diseases can affect kidney function, either directly or indirectly, ranging from acute diseases with reduced filtration as in the case of acute renal failure following massive hemorrhages to chronic diseases with total loss of renal function and architecture as in the case of several autoimmune diseases involving kidney [19]. In particular, metabolic abnormalities in the biochemical pathways of cell metabolism can give rise to severe renal impairment in certain metabolic diseases [20].

Glutaric aciduria type I is a rare metabolic disorder caused by deficiency of the mitochondrial enzyme glutaryl-CoA dehydrogenase (GCDH) [21, 22]. It is a preventable cause of acute brain damage in early childhood, leading to a severe dystonic-dyskinetic disorder. Independent of the neurologic phenotype, kidney function has been shown to significantly decline with age [23]. Gonzalez Melo et al. recently developed a new *Gcdh knock-in* rat model by introducing the mutation p.R402W, the equivalent of the human mutation p.R411W, into the rat *Gcdh* gene. The mutation p.R402W is the most frequent *GCDH* mutation in Caucasians and results in GA-I with a high excretory phenotype. The rat strain was named rat SD-*GCDH*$^{em(R402W)DBA}$ [24]. Gonzalez Melo et al. confirmed a progressive GFR decline and were able to show deterioration of renal architecture in aging knock-in rats (Gonzalez Melo et al., accepted in Molecular Genetics and Metabolism).

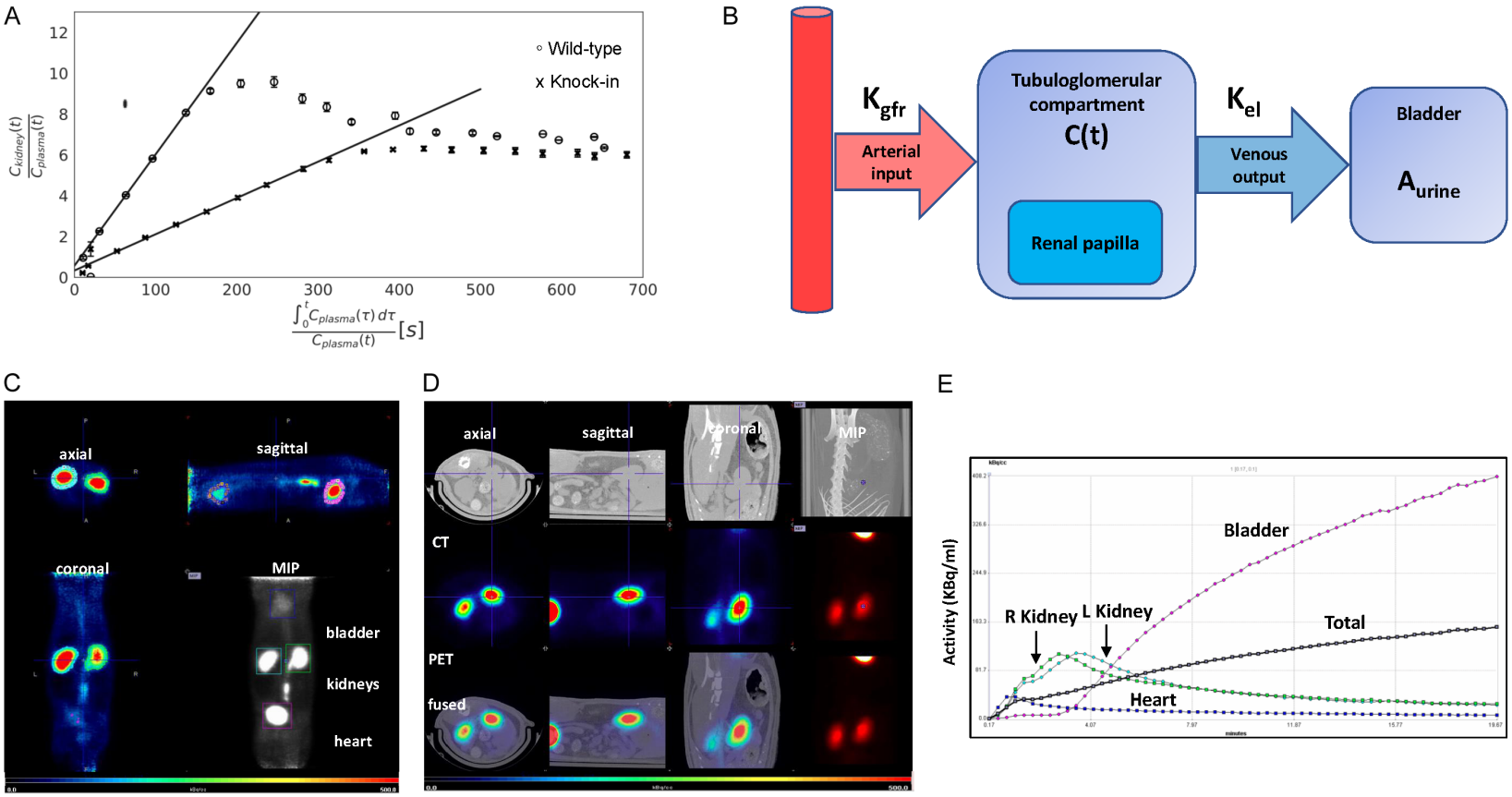

Figure 1. Micro-PET/CT image acquisition and pharmacokinetic modelling using an irreversible unidirectional, two-compartment model. A. A unidirectional, two-compartment model was used to model the kinetic of the cardiac, renal and bladder uptake of the radiotracer and Rutland-Patlak Plot was applied to calculate the filtration constant. In order to assure reduce variance in linear regression analysis, the first 120 seconds were taken into account during model fitting. B. Pharmacokinetic modelling of single-kidney split renal function and perfusion following ^{68}Ga-EDTA administration. The kidney is viewed as two separated compartments, with an external tubule-glomerular compartment and an inner papillary compartment. The filtration and elimination constants are shown. Legend: $C(t)$= concentration at time t, A_{urine} = total bladder activity after end of acquisition (20 minutes), K_{gfr}, = filtration constant, K_{el} = renal elimination constant. C. Region of interest (ROI) of the selected organs based on PET activity signal. The red, central area corresponding approximatively to the inner papillary compartment. D. PET and CT images were acquired separately and superimposed to show co-localization of anatomical and morphological images of both kidneys. E. Resulting time-activity pharmacokinetic curves for the different organs calculated using PMOD derived from the activity in the ROI over a time span of 20 minutes.

In the current study, we validated the use of ^{68}Ga-EDTA as a PET tracer in a longitudinal study by taking advantage of the use of knock-in rats known to develop a decline of renal function with age. Split renal function was calculated by Rutland-Patlak plot and Area Under the Curve analysis to further implement our analysis for determination of the renal function in the scenario of a severe kidney disease.

Material and methods

Tracer synthesis

^{68}Ga was obtained by the elution of a ^{68}Ge/^{68}Ga generator (Eckert & Ziegler, Berlin, Germany) with 0.1 M HCl [25]. The ^{68}Ga-EDTA was then produced by mixing the eluate with 0.05 M EDTA in 0.8 M sodium acetate at pH 5.5 for 5 minutes at room temperature and used without further purification.

Ethics statement

This study was carried out in strict accordance with the ethical principles and guidelines for scientific experiments on animals of the Swiss Academy for the Medical Sciences. The ethics committee for animal experimentation for the canton of Vaud (authorization VD2967.1) approved the protocols. Animals were kept in single ventilated cages and under controlled humidity and temperature (21-23°C), on a 12 h/12 h day/night cycle. Whenever possible, littermate controls were used to compare experimental groups.

Animal experiments

Ten WT animals (5 males and 5 females) and 10 SD-*GCDH*$^{em(R402W)DBA}$ *(knock-in, KI) rats* (5 males and 5 females) were used. Animals were all fed equally with standard diet (SD) and analyzed successively at 6 weeks, 3, 6 and 12 months by PET/CT.

Micro-PET/CT imaging

Dynamic image acquisition was performed right after radiotracer injection in all animals under constant isoflurane anesthesia (4-5% for induction, 1-3% during acquisition time). Ophthalmic gel was applied, and a venous catheter introduced in the caudal vein. Rats were then placed in a micro-PET/SPECT/CT scanner (Albira Si, Bruker, Ettlingen, Germany). Dynamic PET acquisition was started right before injecting animals under the camera with 10 MBq ^{68}Ga-EDTA and was continued for a duration of 20 minutes. Data were generated and framed every 20 seconds using Albira reconstruction software (Albira Si, Bruker, Ettlingen, Germany) to obtain dynamic reconstruction. In order to assess the proper anatomical correlation of the images obtained with ^{68}Ga-EDTA PET, a whole-body, low-dose CT scan was performed on selected rats.

Evaluation of renal function in wild-type and knock-in rats

Images obtained from PET acquisitions were analyzed using the PMOD 3.7 (PMOD Technologies LLC, Zurich, Switzerland). Volumes of interest (VOIs) were placed in the heart, bladder and encompassing both kidneys (without including the renal hilus and the main vessels). The respective time-activity curves were then automatically calculated. Renal volumes for both kidneys were estimated based on PET signal activity. In order to calculate Split Renal Function, we employed two different analytical methodologies, namely Rutland-Patlak Plot analysis and the area under the curve methodology.

The Patlak plot technique describes a two-compartment, unidirectional model with unilateral tracer flow from compartment 1 into compartment 2, where the first compartment models the vascular space, and the second compartment models the nephron space [26]. The basic assumptions in this model are that the A) tracer only flows from compartment 1 into compartment 2, but there is no backflow into compartment 1. B) the interstitial space as a third space is neglected and C) The signal change is directly proportional to the concentration of tracer in a particular voxel at any particular time (**Figure 1B**). The extrarenal background activity in the kidney VOI was then corrected using a perirenal background VOI (**Figure 1C**). The Rutland-Patlak plot is a graphical method for assessing renal function. Let C_{kidney} (t) and C_{plasma} (t) be the tracer concentration at time t in the kidney and plasma, respectively. In a two-compartment model, it can be shown that equation (1) is true after a steady-state time.

The filtration constant of the nephron is extrapolated by plotting the normalized tissue concentration against the normalized integral of the input function.

$$\frac{C_{kidney}(t)}{C_{plasma}(t)} = K_{gfr} * \frac{\int_0^t C_{plasma}(t)}{C_{plasma}(t)} \quad \text{(eq. 1)}$$

Where K_{gfr} corresponds to the radiotracer net influx rate constant. This constant can then be determined by linear interpolation. Results were expressed as averaged values of K_{gfr} for both kidneys for each rat (**Figure 2A** and Supplementary Figure 4A).

Renal Function is calculated by multiplying the K_{gfr} of one kidney by its renal volume (*Vkidney*), and then adding SRF of each kidney to obtain GFR (Equation 2). Because renal clearance is relative to plasma and not total blood, K_{gfr} was multiplied by 0.65, which corresponds to 1-*htc* (hematocrit), whereas rat hematocrit averages at 0.35 [27], and was calculated based on the following (Equation 3):

$$SRF = K_{gfr} * (1 - htc) * V_{kidney} \quad \text{(eq. 2)}$$

In the second method, based on the area under the curve, renal split clearance for the tracer was calculated by the ratio of the total renal excreted activity (bladder VOI at the end of acquisition, which has been set to 20 minutes) and the integral of the plasma curve (glomerulo-tubular AUC), based on the following equation:

$$CL_{tracer} = \frac{A_{urine}(20\text{min})}{\int_0^{20min} A_{plasma}(t)} \quad \text{(eq. 3)}$$

where A_{urine} (20 min) is the total bladder activity after 20 minutes (corresponding to the end of the acquisition window) and $\int_0^{20min} A_{plasma}(t)$ correspond to the Area Under Curve of the blood compartment (heart).

Statistical analysis

Results were expressed as means ± SD. Differences between different groups were assessed by a non-parametric Mann-Whitney test. The significance level was set at $P<0.05$ for all comparisons. Correlation between GFR and RPF was tested using Pearson's correlation coefficient R. Statistic tests were done using GraphPad PRISM 8 (San Diego, USA).

Results

In this study, a detailed time-course analysis of split renal function was carried out from the age of 6 weeks to the age of 12 months in both male and female rats using ^{68}Ga-EDTA PET/CT imaging. We focused particularly our attention on the differences of measurement of renal function between wild-type and knock-in rats [24].

Radiotracer synthesis and image acquisition with PET/CT

The radiochemical yields of the labelling were in the range of >95%, which was routinely achieved as determined by radio HPLC and thin-layer chromatography (TLC). The product solution was stable for at least 3 h after production, enabling direct usage in animals. A total analysis time of 20 minutes at a frame frequency of 20 seconds was chosen to guarantee complete renal filtration and bladder accumulation of the radiotracer for kinetic analysis. In order to assess the proper anatomical correlation of the images obtained with ^{68}Ga-EDTA PET, a whole-body, low-dose CT scan was performed on selected rats followed by image fusion (**Figure 1D**). A proper superimposition between the PET images and the CT images was observed for kidneys, the heart and the bladder.

In vivo tracer distribution and renal plasma filtration measurement

To calculate split renal function for each kidney, tracer distribution was evaluated in kidneys, heart and bladder over the course of 20 minutes. The arterial input function, corresponding to the cardiac curve, showed an initial sharp peak within a few minutes, which can be related to the quick distribution throughout the vascular system following intravenous administration of the tracer, followed by a gradual decrease thereafter. Concomitantly, the ^{68}Ga-EDTA activity in each renal parenchyma was characterized by an initial, steady increase to about 30% of peak value due to initial vascular perfusion followed by a slow rise due to glomerular filtration, finally resulting in a slow decrease as a result of tracer outflow. The bladder kinetic curves showed an initial plateau lasting the time necessary to reach tubular transit, corresponding to time-to-peak, followed

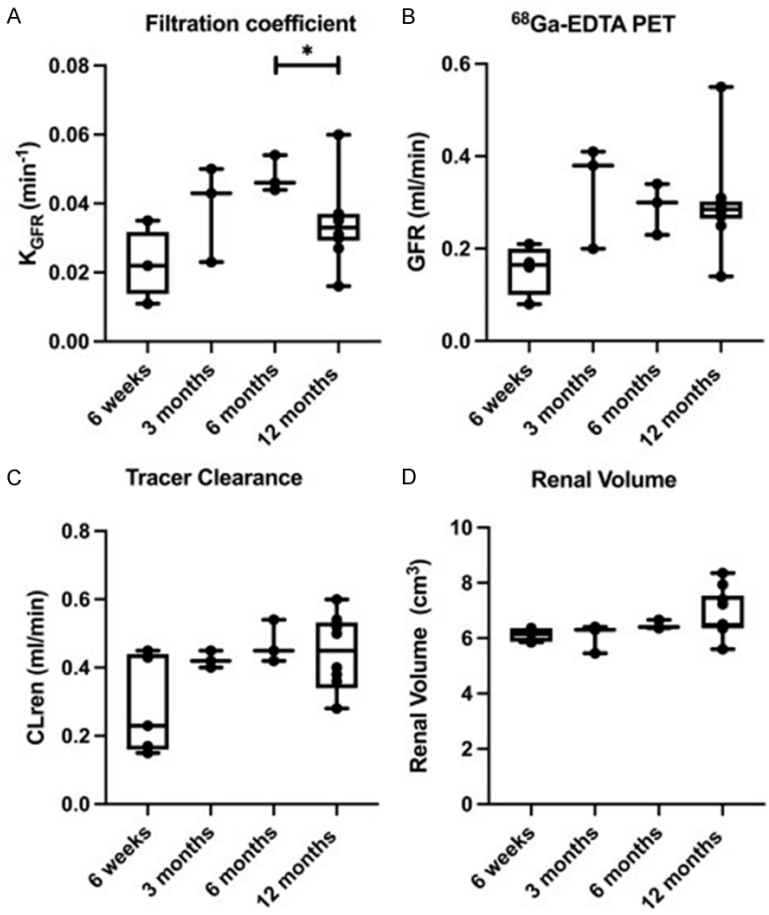

Figure 2. Estimation of pharmacokinetics parameters upon linear regression analysis. A. Glomerular filtration coefficient K_{gfr} was calculated at different time points, ranging from 6 weeks to 12 months, using the linear regression analysis and Patlak-Plot model. B. Corresponding glomerular filtration rate (GFR), which is proportional to the filtration coefficient and the renal volume, based on PET activity. C. Clearance of the radiotracer at different time points ranging from 6 weeks to 12 months, corresponding to the ratio of the total renal excreted activity (bladder VOI at the end of acquisition, set to 20 minutes) and the integral of the plasma curve (tubule-glomerular AUC). D. Renal volume over the lifespan of the animals, expressed as the average of both left and right kidneys. Volume calculation was based on distribution of tracer activity in the ROI and performed automatically by the PMOD software. Significant differences P<0.05 are indicated by (*).

by a rapid and constant increase as a result of tracer inflow (**Figure 1E**). Detailed time-to-peak analysis was evaluated for each renal curve, averaging at 145±25 sec for wild-type and 150±27 for knock-in animals (Supplementary Figure 1). Linear regression analysis of the Rutland-Patlak plot to calculate the filtration rate showed a significant increase from 0.025±0.01 ml/min at 6 weeks to 0.049±0.05 ml/min at 6 months followed by a slight decrease to 0.33±0.01 ml/min at 12 months (**Figure 2A**) with a very good fit, as evidenced by R-squared values, averaging 0.985±0.0084 for wild-type rats and 0.098±0.0024 for knock-in rats (Supplementary Figure 2). No significant difference between right and left kidneys K_{gfr} was observed (Supplementary Figure 3A). Glomerular filtration, which is proportional to renal volume, increased from 0.15±0.05 ml/min at 6 weeks to 0.32±0.05 ml/min at 3 months and remained constant throughout the life of the animals (**Figure 2B**). Analysis of renal volume showed already fully formed kidneys at 6 weeks, with a volume of 6.23±0.27 cm^3 that remained constant throughout the life of the animal (**Figure 2C**).

When looking at each kidney individually, no significant difference between right and left kidney volumes was observed in the animals (P=0.68, Supplementary Figure 3B). To further characterize renal filtration, tracer clearance (CL_{tracer}) that is directly related to the renal plasma flow was determined. Similar to glomerular filtration rate, tracer clearance increased steadily over time, ranging from 0.27±0.13 ml/min at 6 weeks to 0.47±0.11 ml/min at 6 months (**Figure 2D**).

Detection of progressive renal impairment in knock-in rats

To validate the use of ^{68}Ga-EDTA PET/CT imaging in an animal model of chronic kidney disease, WT and KI rats were imaged starting at the age of 6 weeks (**Figure 3A**). No significant difference was observed in renal volumes between KI and WT animals, based on imaging-derived volume calculations (**Figure 3B**). Rutland-Patlak plot analysis of KI^i versus WT rats showed a significantly lower signal intensity in KI animals compared to WT at 3, 6 and 12

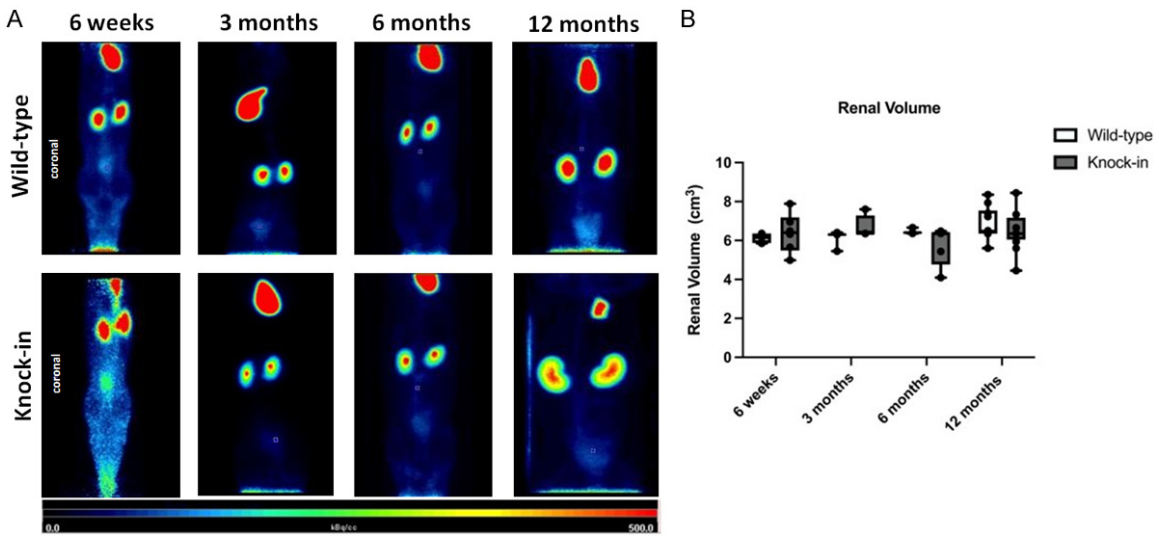

Figure 3. Representative PET-CT images at the different time points investigated in the study and activity-based volume assessment in both wild-type and knock-in animals. A. PET signal activity in selected rats at different time points, ranging from 6 weeks to 12 months, showing both renal, bladder and cardiac activity. ROIs were then modelled around the activity regions and the different parameters determined using linear regression. B. Renal volume over the lifespan of the animals for wild-type and knock-in rats, calculated from PET signals. Values are averaged from both left and right kidneys.

months (0.033 min^{-1} vs. 0.01 min^{-1}, P<0.001), with no difference observed between right and left kidney volumes (P=0.98, **Figure 4A** and Supplementary Figure 4A). Similarly, glomerular filtration was significantly lower in KI animals compared to WT animals at 3, 6 and 12 months (0.29 ml/min^{-1} vs. 0.045 ml/min^{-1}, P<0.0001), with no significant difference between right and left kidney at 3 months (P=0.73, **Figure 4B** and Supplementary Figure 4B). Interestingly, tracer clearance in KI rats showed a marked increase from 0.22 ml/min^{-1} at 6 weeks to 0.36 ml/min^{-1} at 3 months, followed by a rapid decrease at 0.15 ml/min^{-1} at 6 and 12 months, unlike WT animals (**Figure 4C**).

Finally, we performed plasmatic elimination kinetic (K_{el}) of ^{68}Ga-EDTA by analyzing the final portion (ranging from 800 to 1200 seconds) of the renal elimination curve. K_{el} was reduced in KI animals at 12 months compared to WT animals (0.0014±0.00015 min^{-1} versus 0.0009± 0.0002 min^{-1}, P<0.01) but not at 6 weeks (P=0.17, **Figure 4D**).

Discussion

In the present study we have investigated the use of ^{68}Ga-EDTA PET/CT imaging for renal function in an animal model known to present a progressive decline of renal function [23]. We have employed Rutland-Patlak Plot analysis to determine the glomerular filtration rate, which represent the integrity of renal filtration for ^{68}Ga-EDTA as this tracer is neither actively secreted nor resorbed. Typically, a peak renal AUC was observed within the first few minutes post injection, therefore we concluded that ^{68}Ga-EDTA is trapped in the kidney during the first minutes, allowing the mathematical use of the Rutland-Patlak plot analysis to glomerular filtration. To our knowledge there is currently no clear consensus concerning the exact time interval used for regression analysis in the Rutland-Patlak Plot. We therefore opted for starting the interval at 30 seconds to rule out any differences in the vascular distribution of the tracer between animals. The end of the evaluation interval was set at 90 seconds, as after this time a decrease in data values in the renal filtration occurred, probably due to the elimination of the radiopharmaceutics into the urinary bladder. This interval allowed us to obtain reliable results, as observed by the determination coefficient (R^2). Notably, our analysis evidenced an increase in renal filtration corresponding to the growth pattern of animal according to its age, but also a slight but significant decrease in the filtration coefficient from 6 months to 12 months, which could have several explana-

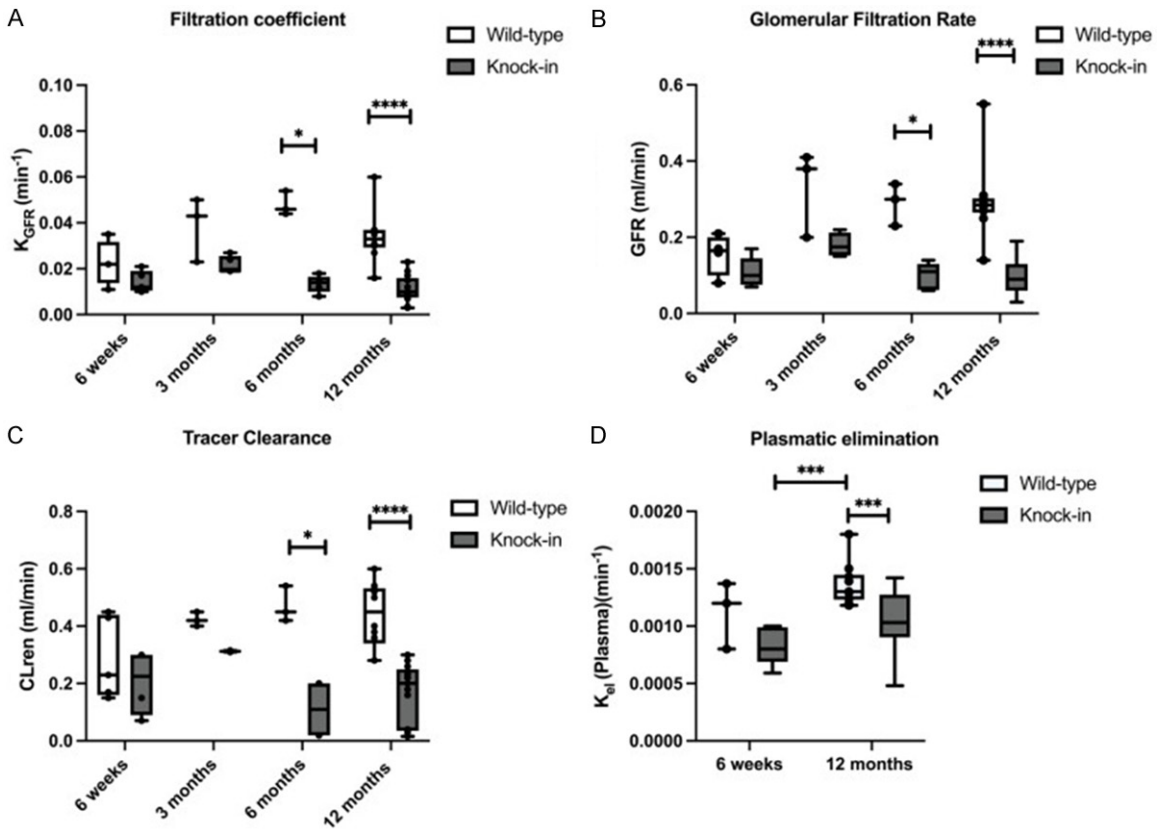

Figure 4. Estimation of pharmacokinetics parameters upon linear regression analysis in knock-in animals compared to wild-type animals. A. Glomerular filtration coefficient K_{gfr} was calculated at different time points, ranging from 6 weeks to 12 months, using the linear regression analysis and Patlak-Plot model for both wild-type and knock-in rats. B. Corresponding glomerular filtration rate (GFR), which is proportional to the filtration coefficient and the renal volume, based on PET activity for both wild-type and knock-in rats. C. Clearance of the radiotracer at different time points ranging from 6 weeks to 12 months, corresponding to the ratio of the total renal excreted activity (bladder VOI at the end of acquisition, set to 20 minutes) and the integral of the plasma curve (tubule-glomerular AUC) for both wild-type and knock-in rats. D. Renal volume over the lifespan of the animals for both wild-type and knock-in rats, expressed as the average of both left and right kidneys. Significant differences are indicated by *P<0.05, ***P<0.01 and ****P<0.0001.

tions. We assumed the decrease observed in renal filtration might be due to a physiological reduction in the glomerular capacity presenting with the advancing aging of the animals, and not a reduction in effective renal volume. Unfortunately, we were not able to properly collect enough urine samples to perform creatinine analysis to assess renal function over time, nor to perform post-mortem biopsies to properly quantify renal volume on all animals. Nevertheless, we adopted another approach consisting of calculating AUCs and deriving plasma filtration rate. The obtained ^{68}Ga-EDTA clearance showed linear correlation (Spearman's correlation coefficient of 0.898, P<0.01) with Rutland-Patlak plot analysis and therefore glomerular filtration (Supplementary Figure 5).

We then turned our interest to analyze renal function in KI rats known to have kidney impairment because of a deteriorating metabolic disease (Melo et al. Knock-in rat model unravels acute and chronic renal toxicity in glutaric aciduria type I. *In preparation*). Notably, these KI animals never reached the renal filtration capacity observed in wild type animals. Notably, KI rats showed significantly reduced GFR and RPF at the age of 6 and 12 months compared to wild type rats, while no change of renal volumes were observed. Concomitantly, we could observe a diminished plasma elimination rate

at 12 months, which might indirectly be an indicator of a reduced ^{68}Ga-EDTA plasmatic clearance.

The main limitations of the current study were the defined numbers of animals we were able to analyze, and the number of time points assessed. We did start our analysis at 3 weeks, but due to the very young age and size of the animals, we were not able to obtain proper images. As mentioned before, we were not able to collect urine samples or renal biopsies at each time point to have a direct look at renal function over time.

In summary, our study presents a simple and reliable methodology to assess total and single kidney GFR and renal plasma filtration from a single dynamic ^{68}Ga-EDTA PET. We thus showed that ^{68}Ga-EDTA is a reliable tracer to analyze split renal function in rats using PET/CT. For animal usage, kidney VOI based on a PET acquisition time of around twenty minutes was largely sufficient. These results could be translated into practical clinical application of ^{68}Ga-EDTA PET in human patients, which would allow an estimation of kidney function parameters by a routine PET scan and would be suitable for evaluation of patients with renal failure.

Acknowledgements

MicroPET/SPECT/CT acquisitions and analysis were conducted at the nuclear medicine research laboratory and at the in vivo imaging facility (IVIF) at the Lausanne University Hospital and University of Lausanne.

Disclosure of conflict of interest

None.

Abbreviations

AUC, Area Under the Curve; EDTA, ethylendiamminiumtetra-acetate; GFR, Glomerular Filtration Rate; GCDH, (mitochondrial) glutaryl-CoA dehydrogenase; K_{gfr}, Filtration Constant; PET, Positron Emission Tomography; RPF, Renal Plasma Flow.

Address correspondence to: Dr. John O Prior, Department of Nuclear Medicine and Molecular Imaging, Lausanne University Hospital and University of Lausanne, Rue du Bugnon 46, CH-1011 Lausanne, Switzerland. Tel: +41-079 556 8702; Fax: +41-021314434; E-mail: john.prior@chuv.ch

References

[1] Levey AS, Coresh J, Tighiouart H, Greene T and Inker LA. Measured and estimated glomerular filtration rate: current status and future directions. Nat Rev Nephrol 2020; 16: 51-64.
[2] Levey AS, Perrone RD and Madias NE. Serum creatinine and renal function. Annu Rev Med 1988; 39: 465-90.
[3] Rose GA. Measurement of glomerular filtration rate by inulin clearance without urine collection. Brit Med J 1969; 2: 91-3.
[4] Janssen WM, Beekhuis H, de Bruin R, de Jong PE and de Zeeuw D. Noninvasive measurement of intrarenal blood flow distribution: kinetic model of renal 123I-hippuran handling. Am J Physiol 1995; 269: F571-80.
[5] Clausen TD, Kanstrup I and Iversen J. Reference values for 99mTc-MAG3 renography determined in healthy, potential renal donors. Clin Physiol Funct I 2002; 22: 356-60.
[6] Delbeke D, Schöder H, Martin WH and Wahl RL. Hybrid imaging (SPECT/CT and PET/CT): improving therapeutic decisions. Semin Nucl Med 2009; 39: 308-40.
[7] Werner RA, Chen X, Lapa C, Koshino K, Rowe SP, Pomper MG, Javadi MS and Higuchi T. The next era of renal radionuclide imaging: novel PET radiotracers. Eur J Nucl Med Mol I 2019; 46: 1773-86.
[8] Roca I, Simó M, Sábado C and de Toledo JS. PET/CT in paediatrics: it is time to increase its use! Eur J Nucl Med Mol I 2007; 34: 628-9.
[9] Hofman MS and Hicks RJ. Gallium-68 EDTA PET/CT for renal imaging. Semin Nucl Med 2016; 46: 448-61.
[10] Hofman M, Binns D, Johnston V, Siva S, Thompson M, Eu P, Collins M and Hicks RJ. 68Ga-EDTA PET/CT imaging and plasma clearance for glomerular filtration rate quantification: comparison to conventional 51Cr-EDTA. J Nucl Med 2015; 56: 405-9.
[11] Ilsen HW, Sato M, Pawlik G, Herholz K, Wienhard K and Heiss WD. (68Ga)-EDTA positron emission tomography in the diagnosis of brain tumors. Neuroradiology 1984; 26: 393-8.
[12] Jiang D, Ge Z, Im HJ, England CG, Ni D, Hou J, Zhang L, Kutyreff CJ, Yan Y, Liu Y, Cho SY, Engle JW, Shi J, Huang P, Fan C, Yan H and Cai W. DNA origami nanostructures can exhibit preferential renal uptake and alleviate acute kidney injury. Nat Biomed Eng 2018; 2: 865-77.
[13] Damasio MB, Bodria M, Dolores M, Durand E, Sertorio F, Wong MCY, Dacher JN, Hassani A, Pistorio A, Mattioli G, Magnano G and Vivier PH. Comparative study between functional MR urography and renal scintigraphy to evaluate drainage curves and split renal function in children with congenital anomalies of kidney and

urinary tract (CAKUT). Front Pediatr 2020; 7: 527.
[14] Claudon M, Durand E, Grenier N, Prigent A, Balvay D, Chaumet-Riffaud P, Chaumoitre K, Cuenod CA, Filipovic M, Galloy MA, Lemaitre L, Mandry D, Micard E, Pasquier C, Sebag GH, Soudant M, Vuissoz PA and Guillemin F; DCE MR Urography Study Group. Chronic urinary obstruction: evaluation of dynamic contrast-enhanced MR urography for measurement of split renal function. Radiology 2014; 273: 801-12.
[15] Rohrschneider WK, Hoffend J, Becker K, Clorius JH, Darge K, Kooijman H and Tröger J. Combined static-dynamic MR urography for the simultaneous evaluation of morphology and function in urinary tract obstruction. Pediatr Radiol 2000; 30: 511-22.
[16] Grenier N, Cornelis F, Bras YL, Rigou G, Boutault JR and Bouzgarrou M. Perfusion imaging in renal diseases. Diagn Interv Imag 2013; 94: 1313-22.
[17] Mehl JN, Lüpke M, Brenner AC, Dziallas P, Wefstaedt P and Seifert H. Measurement of single kidney glomerular filtration rate in dogs using dynamic contrast-enhanced magnetic resonance imaging and the Rutland-Patlak plot technique. Acta Vet Scand 2018; 60: 72.
[18] Al-Shakhrah IA. A comparison of deconvolution and the Rutland-Patlak plot in parenchymal renal uptake rate. Indian J Nucl Med 2012; 27: 176-80.
[19] Ferenbach DA and Bonventre JV. Acute kidney injury and chronic kidney disease: from the laboratory to the clinic. Nephrol Ther 2016; 12 Suppl 1: S41-8.
[20] El-Hattab AW. Inborn errors of metabolism. Clin Perinatol 2015; 42: 413-39.
[21] Jafari P, Braissant O, Bonafé L and Ballhausen D. The unsolved puzzle of neuropathogenesis in glutaric aciduria type I. Mol Genet Metab 2011; 104: 425-37.
[22] Barić I, Zschocke J, Christensen E, Duran M, Goodman SI, Leonard JV, Müller E, Morton DH, Superti-Furga A and Hoffmann GF. Diagnosis and management of glutaric aciduria type I. J Inherit Metab Dis 1998; 21: 326-40.
[23] Pöge AP, Autschbach F, Korall H, Trefz FK and Mayapetek E. Early clinical manifestation of glutaric aciduria type I and nephrotic syndrome during the first months of life. Acta Paediatr 1997; 86: 1144-7.
[24] Melo MG, Remacle N, Cudré-Cung HP, Roux C, Poms M, Cudalbu C, Barroso M, Gersting SW, Feichtinger RG, Mayr JA, Costanzo M, Caterino M, Ruoppolo M, Rüfenacht V, Häberle J, Braissant O and Ballhausen D. The first knock-in rat model for glutaric aciduria type I allows further insights into pathophysiology in brain and periphery. Mol Genet Metab 2021; 133: 157-181.
[25] Schmaljohann J, Schnitzler J, Morgenroth A and Mottaghy F. Preparation of 68Ga-EDTA ready for injection as a PET-imaging probe for measuring the glomerular filtration rate. J Nucl Med 2011.
[26] Hackstein N, Kooijman H, Tomaselli S and Rau WS. Glomerular filtration rate measured using the Patlak plot technique and contrast-enhanced dynamic MRI with different amounts of gadolinium-DTPA. J Magn Reson Imaging 2005; 22: 406-14.
[27] Dewey WC. Distribution and hematocrit ratios of blood in the rat. Am J Physiol 1960; 198: 1011-3.

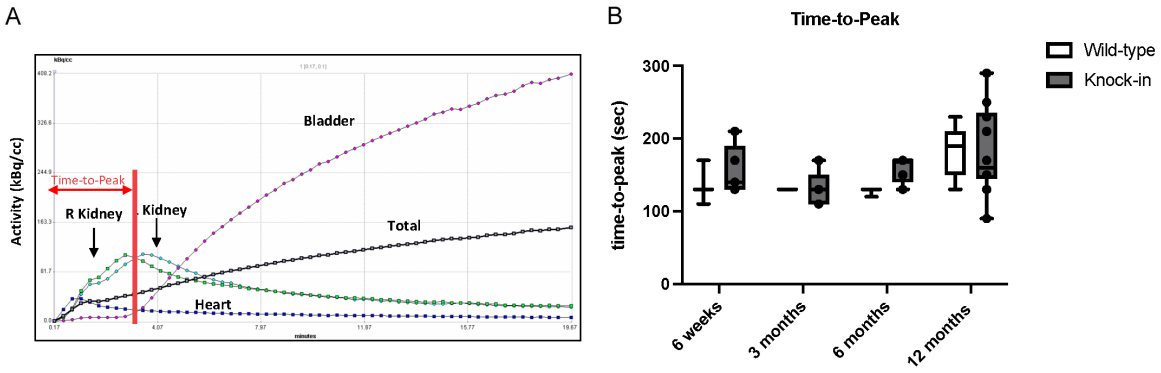

Supplementary Figure 1. Time-to-peak analysis for renal time-activity pharmacokinetic curve. A. Graphical representation of the methodology used to evaluate time-to-peak based on time-activity curve. B. Average time-to-peak for both right and left kidney was calculated at different time points, ranging from 6 weeks to 12 months, by assessing the time to reach maximal tracer activity in wild-type and knock-in rats.

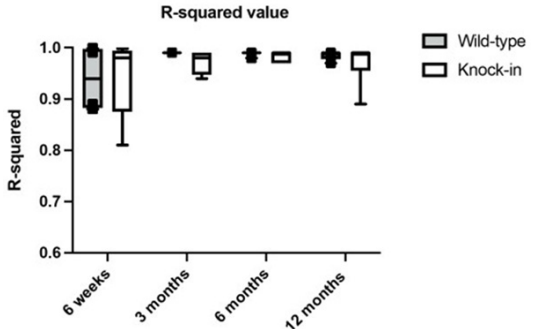

Supplementary Figure 2. Statistical variance for Rutland-Patlak-Plot analysis. R-squared values from linear regression analysis on Rutland-Patlak Plot were calculated independently for both right and left kidneys and averaged among wild-type and knock-in animals at every time points, ranging from 6 weeks to 12 months (0.985±0.0084 for wild-type rats and 0.098±0.0024 for knock-in rats).

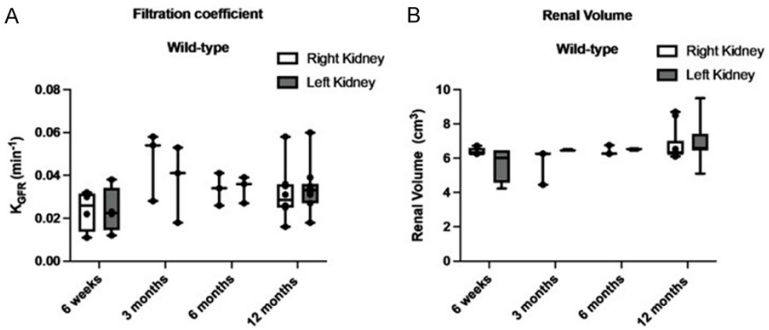

Supplementary Figure 3. Estimation of pharmacokinetics parameters for upon linear regression analysis in wild-type animals. A. Glomerular filtration coefficient K_{gfr} was calculated at different time points, ranging from 6 weeks to 12 months, using the linear regression analysis and Patlak-Plot model for each kidney separately in wild-type animals. B. Right and left renal volume in wild-type rats. Volume calculation was based on distribution of tracer activity in the ROI and performed automatically by the PMOD software.

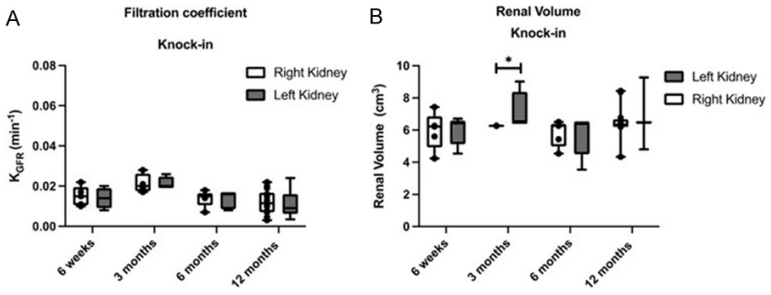

Supplementary Figure 4. Estimation of pharmacokinetics parameters for upon linear regression analysis in knock-in animals. A. Glomerular filtration coefficient K_{gfr} was calculated at different time points, ranging from 6 weeks to 12 months, using the linear regression analysis and Patlak-Plot model for each kidney separately in knock-in animals. B. Right and left renal volume in wild-type rats. Volume calculation was based on distribution of tracer activity in the ROI and performed automatically by the PMOD software.

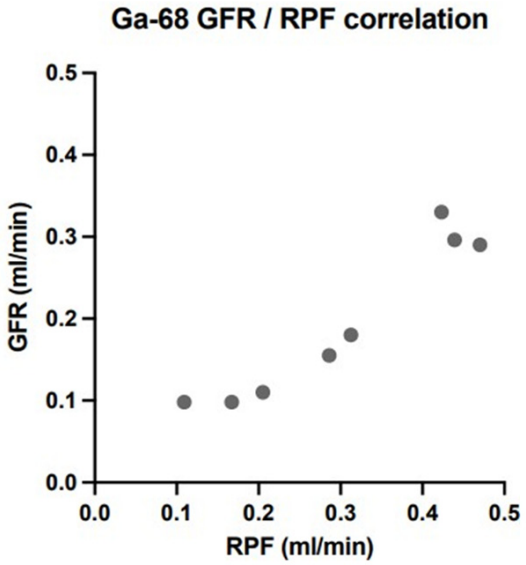

Supplementary Figure 5. Linear correlation between Glomerular Filtration Rate and Renal Plasma Flow. Values for Glomerular Filtration Rate (GFR) and Renal Plasma Flow (RPF) for wild-type and knock-in animals between 6 weeks and 12 months, each data point corresponding to a specific time and either wild-type and knock-in animals. A Spearman Correlation of 0.898 ($P<0.01$) was obtained from statistical analysis.